Article ID: 1004-924X(2001)05-0418-06

Development of an Experimental EUVL System

JIN Chun-shui, MA Yue-ying, PEI Shu, CAO Jian-lin

(*Changchun Institute of Optics, Fine Mechanics and Physics, Chinese Academy of Sciences, Changchun* 130022, *China*)

Abstract: The authors have developed an experimental system for the studies of extreme ultraviolet projection lithography at 13.0nm wavelength, which includes a laser plasma source, an ellipsoidal condenser, a transmission mask and a Schwarzschild optics. The optical system is optimized to achieve 0.1μm resolution over a 0.1mm diameter image field of view and the mirrors of the objective were coated with Mo/Si multilayer to provide 60% reflectance at near-normal incidence angle for 13.0nm radiation.

Key words: extreme ultraviolet projection lithography; multilayer reflectors; Schwarzschild optics

CLC number: TN305.7 **Document code:** A

1 Introduction

Extreme ultraviolet lithography (EUVL) is expected as a candidate for VLSI production in the near future. Reduction optics with aspherical mirror of sub-nanometer accuracy are required to get a resolution of less than 0.1μm and wide exposure area simultaneously[1-2]. The precision of polishing and testing for such aspherical surface is fairly high and it has not been achieved yet in our current state. It might be preferable, however, to use spherical mirror for the first step studies of EUVL in a serial investigation of system design, component fabrication, assembly technique and experimental process[3-4].

Along this thought, we developed a 10:1 reduction imaging system using molybdenum/silicon (Mo/Si) multilayer coated Schwarzschild optics. The imaging experiments are being carried out with transmission mask and 13.0nm EUV radiation from a laser plasma source.

2 General configuration of the experimental EUVL system

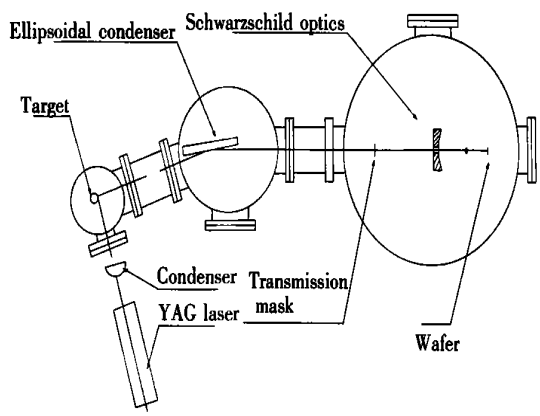

Fig. 1 Configuration of the experimental arrangement for EUVL

Received date: 2001-08-29; **revised date:** 2001-10-08

Figure 1 is the configuration of elementary arrangement of our experimental EUVL system. Laser plasma source (LPS) is composed of a YAG laser with 0.8J pulse energy, 10Hz frequency and 10ns pulse width, and vertiginous copper target. By a condenser of 200mm focal length, the laser is focused onto the copper target through a fused quartz window. The laser spot has a diameter of about 200μm and achieves a 0.8% conversion efficiency from laser energy to EUV radiation in a 2.5% bandwidth centered at 13.0nm[4]. In order to get steady EUV radiation, the target revolves at certain speed according to the operating frequency of the laser pulse. The LPS-generated EUV illuminates the transmission mask through grazing ellipsoidal condenser, and then the illuminated mask produces a 10-times minified image on a resist-coated silicon wafer through a Schwarzschild optics, of which the mirror optics are coated with Mo/Si multilayer.

The ellipsoidal condenser was designed according to the equation

$$\frac{x^2}{354^2} + \frac{y^2 + z^2}{55^2} = 1 \qquad (1)$$

and its numerical aperture is larger than 0.02 with the distance from the illuminated spot on copper target to the condenser and from the condenser to the transmission mask of 231mm and 469mm, respectively. It was polished and then coated with nickel phosphorus at the optical workshop of our institute.

The influence of the roughness on reflectance of the surface could be evaluated by Debye-Waller factor

$$R = R_0 \exp\left[-\left(4\pi\sigma\sin\Phi/\lambda\right)^2\right] \qquad (2)$$

here R and R_0 are the reflectance of the surface and ideal surface ($\sigma = 0$), respectively, σ is the RMS roughness of the surface, Φ is the grazing incidence angle, and λ is the wavelength of the incident radiation. Fig. 2 shows the calculated results of reflectance (R) vs. grazing incidence angle (Φ) with different surface roughness (σ) from up to down of 0, 1, 3, and 5nm at 13.0nm wavelength for nickel phosphorus surface. We can know that the surface roughness has no large influence on the reflectance, provided that it is less than 1nm in the region of a small grazing incidence angle.

Fig. 3 shows the measured roughness of the ellipsoidal condenser by a WYKO interferometer. The reflectance of the condenser is therefore evaluated to be more than 50% for the grazing incidence angle smaller than 8.5° at 13.0nm wavelength, since the measured roughness (RMS) is less than 1nm.

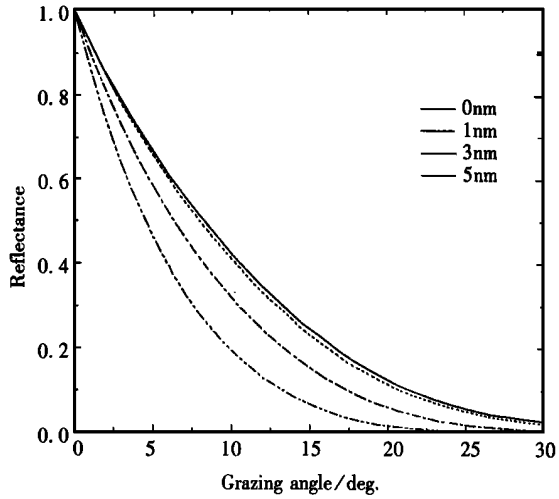

Fig. 2 Reflectance of Ni as grazing angle and roughness

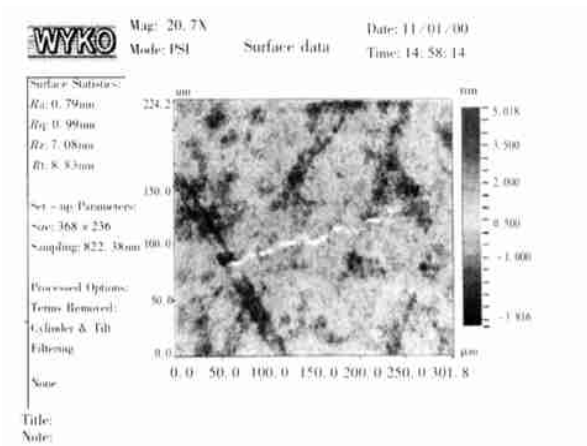

Fig. 3 Roughness of condenser mirror measured by WYKO

In our configuration, it is rather difficult to find the optimum position of imaging plane because the designed focus depth is only about 1μm. On the contrary, it is much more easier for the focusing

alignment of mask as the longitudinal magnification is the square of the transverse one. Therefore we fixed the imaging plane and employed a stage with linearity of 0.3μm and resolution better than 1μm to align the mask.

3 Design of Schwarzschild optics

The two-mirror Schwarzschild system that can correct the third-order spherical aberration, coma, and astigmatism should satisfy the Schwarzschild condition,

$$\frac{a}{(a-1)^2} = \frac{(1+M)^2}{(1-M)^2} \tag{3}$$

with the magnification rate

$$M = -\frac{R_1 R_2}{2R_1 L_0 - R_1 R_2 - 2R_2 L_0} \tag{4}$$

here $a = R_1/R_2$, and R_1, R_2 is the curvature radius of the primary and secondary mirror, respectively. L_0 is the distance between the primary mirror to the transmission mask. The layout of Schwarzschild optics is shown in Fig. 4.

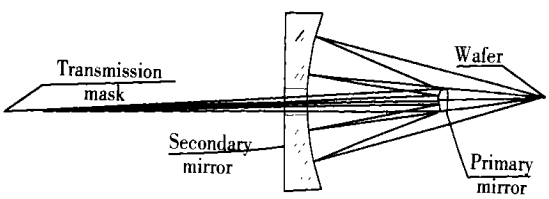

Fig. 4 Layout of Schwarzschild optics.

Among the four parameters (R_1, R_2, M, and L_0) in (3) and (4), there are only two independent ones for optimizing. In our design we chose M (= 0.1) and R_2 (= 101.1 mm), and determined R_1 and L_0 through optimization calculation. The design results are listed in Table1. The consideration of curvature radius mainly comes from the multilayer deposition process, because it is difficult to get uniform coating for too small curvature radius. On the other hand, the dimensional limitation of our instruments and facilities also restricts the utilization of large curvature radius.

Table 1 Characteristics of Schwarzschild optics

Magnification	0.1
Numerical aperture	0.2
Object distance	231.533mm
Distance between the two mirrors	69.473mm
Imaging distance	126.461mm
Primary mirror	diameter 8mm, radius of curvature 31.48mm
Secondary mirror	diameter 80mm, radius of curvature101.1mm
Diffraction limit	0.065μm
Residual wave-front error of design	0.007λ(λ= 13nm)

Fig. 5 gives the calculated modulation transfer function (MTF) of our Schwarzschild optics. The result shows that resolution of 0.1μm can be achieved for an image field of 0.1mm in diameter. In this analysis we also know that there are still some high-order aberrations which affect the imaging performance of the system, for example, the fifth-order spherical aberration, oblique spherical aberration, coma, and astigmatism limit the numerical aperture and usable image field.

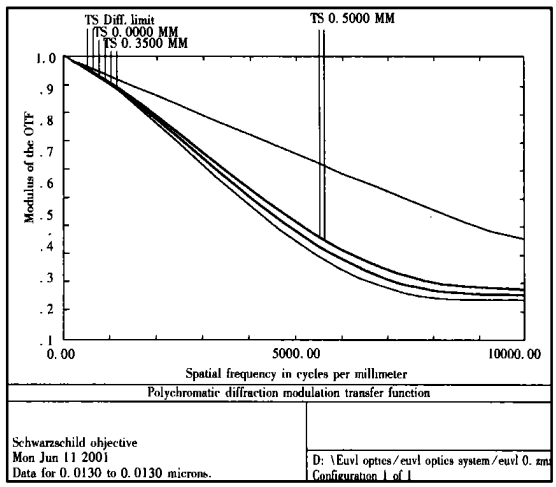

Fig. 5 Calculated modulation transfer function for Schwarzschild optics.

4 Fabrication of optical components of Schwarzschild optics

For the purpose of obtaining high resolution up to diffraction limitation, the figure error at-

tributed to each optical component can be expressed by Rayleigh formula (5) and Marechal formula (6):

$$\delta_1 = \lambda/4n \quad (\mathrm{PV}) \qquad (5)$$

$$\delta_2 = \lambda/28\sqrt{n} \quad (RMS) \qquad (6)$$

here n is the number of optical components in the system and λ is the operating wavelength. For two-mirror projection system operating at 13nm, the PV and RMS figure error in each mirror should be less than 2nm and 0.5nm, respectively.

Furthermore, the surface roughness of the optical component is also a key factor, which affects the reflectance of multilayers and the quality of imagery. By using (2) in the case of normal incidence ($\Phi = 90°$), we can know that if we hope to reduce the scattering loss to a level less than 10%, the RMS surface roughness should be smaller than $\lambda/40$, which reaches a scale of deep-subnanometer. As the surface/ intersurface roughness of multilayer is generally similar to that of substrate, the surface roughness of substrates should also be less than $\lambda/40$.

We employed a ZYGO and a WYKO interferometer to measure the surface figure error and roughness, respectively, for both primary and secondary mirror substrate polished in our lab. Fig. 6 and Fig 7 give the results for the secondary mirror. The results show that both δ_2 (about 5nm) and σ (about 0.7nm) are still far from the requirement of high resolution given in (6) and (2).

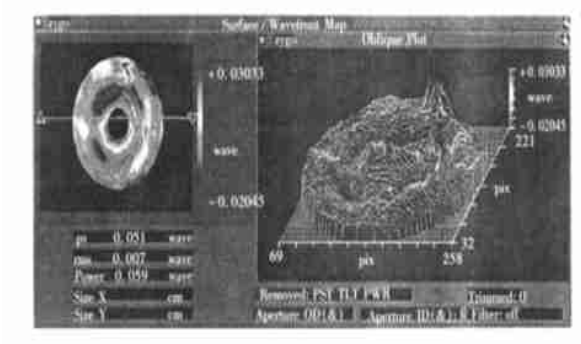

Fig. 6 Measured figure error of the secondary mirror with Zygo Mark Ⅳ

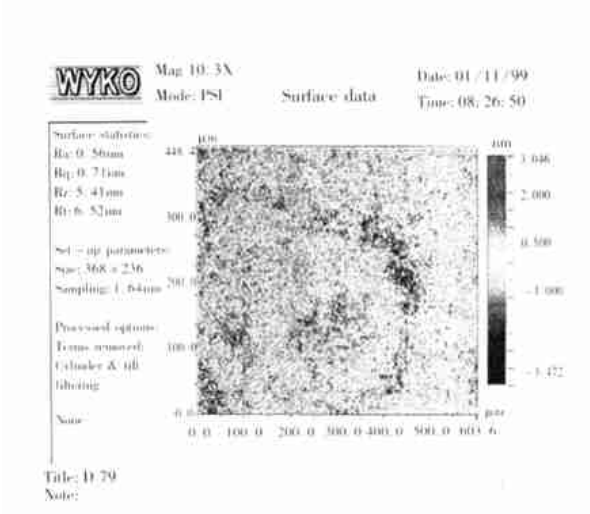

Fig. 7 Measured roughness of the secondary mirror with WYKO

The EUV multilayer could be analyzed as an artificial one-dimensional Bragg structure. Ignoring the refraction and absorption effect, the reflection peak of EUV multilayer can be medicated by Bragg equation:

$$K\lambda = 2N d\cos\theta \qquad (7)$$

here k is the diffraction order, N is the equivalent refractive index of one pair (period) layer, θ is the angle of incidence, $d(= d_1 + d_2)$ is the period thickness, and d_1, d_2 are the thickness of single layer for two coating material, respectively. Formula (7) shows that the spectral response of a multilayer with period thickness d depends upon both the angle of incidence and the wavelength of the radiation. During the radiation's passing through the system, the angles of incidence on the primary and secondary mirror are different, and they vary across each mirror surface as well, while the d spacing of multilayer is constant across each mirror surface. The reflectance peak moves, therefore, as the angle of incidence varies. Fig. 8 shows the calculated reflectance vs. wavelength of the primary and secondary mirror for three different rays, one central and two extreme margins by using the optical constants of the Center for X-ray Optics, Lawrence Berkeley National Laboratory[5]. The d spacing for the calculation in Fig. 8 (a) and Fig. 8

(b) is 6.7nm and 6.63nm, respectively, and these two values are the results of our multilayer design aiming at same reflectance peak of 13.0nm (95.4eV) for both primary and secondary mirrors. According to Fig. 8, the peak of reflectance changes in a small scale on the scope of incident angle we confined. Fig. 8 also shows that it is unnecessary to deposit multilayer with graded d spacing in the present case.

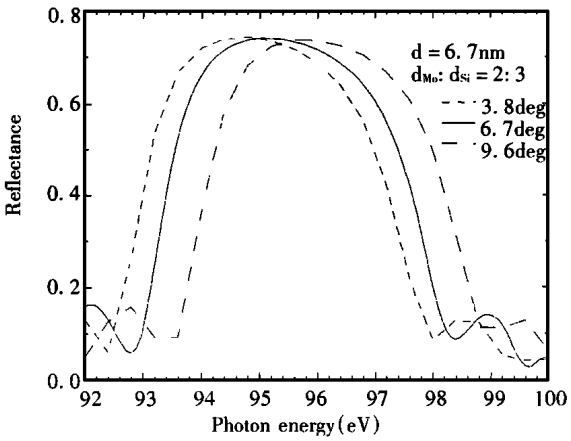

(a) Primary mirror

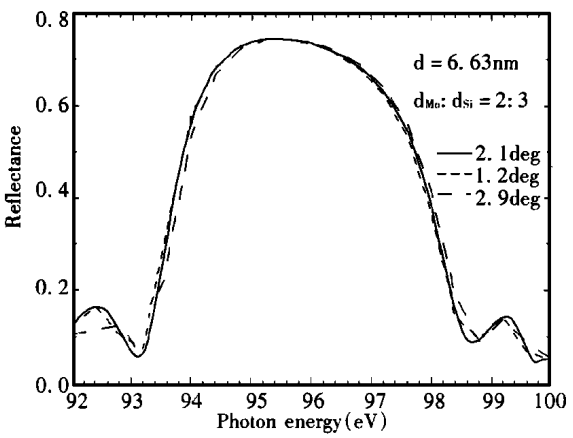

(b) Secondary mirror

Fig. 8 Calculated reflectance of the Mo/Si multilayer coatings is applied to the mirrors of Schwarzschild optics. Curves are shown for the central ray and the two extreme rays pass the system.

We deposited 81-layer Mo/Si multilayer (both bottom and top layers were Mo) on the primary and secondary mirror with d= 6.7nm (d_{M_0} = 4.02 nm, d_{Si} = 2.68 nm) by using our ion beam sputtering facilities. The reflectance of the multilayer was measured by a reflectometer with LPS. Fig. 9 shows the result and it can be seen that the reflectance reaches 60% and well centralizes at 13nm.

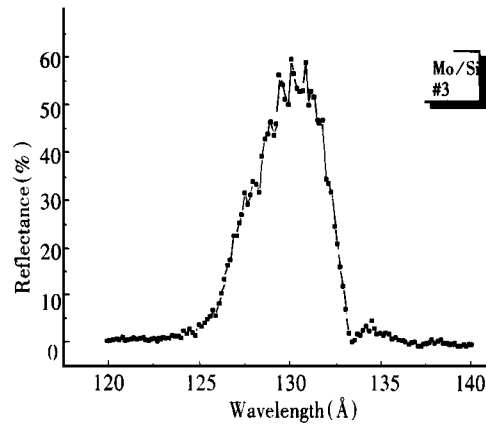

Fig. 9 Measured reflectivity of the primary and secondary mirrors

5 Computer-aided alignment of Schwarzschild optics

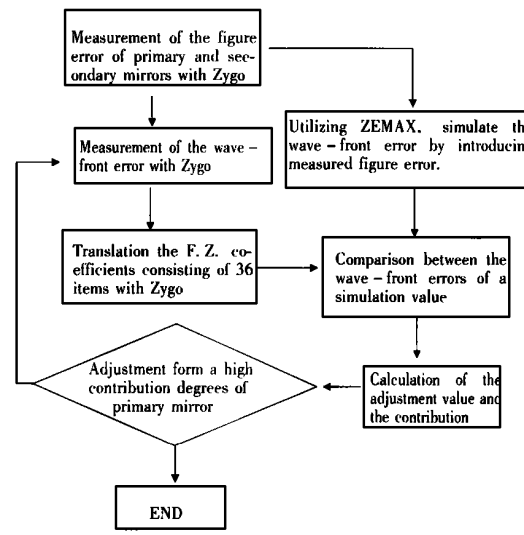

Fig. 10 Flow diagram of the computer aided alignment for Schwarzschild optics.

Another key technical factor for EUVL is the accuracy in assembly and/or alignment of the optical system. From formulas (5) and (6), we know that the maximum error produced by assembly process should be in the order of nanometer for a system operating at 13.0nm wavelength. We intro-

duced a computed-aided alignment to such challenge. Fig. 10 shows the flow diagram and Fig. 11 is the instrumentation layout. Under the guidance of simulating calculation, we finished the assembly of the Schwarzschild optics with the total wave front error of 0.025 λ (λ = 632.8nm). Fig. 12 gives the result. Comparing Fig. 12 with Fig. 6, it is found that the main error of the system is the fabrication one existing in polishing process.

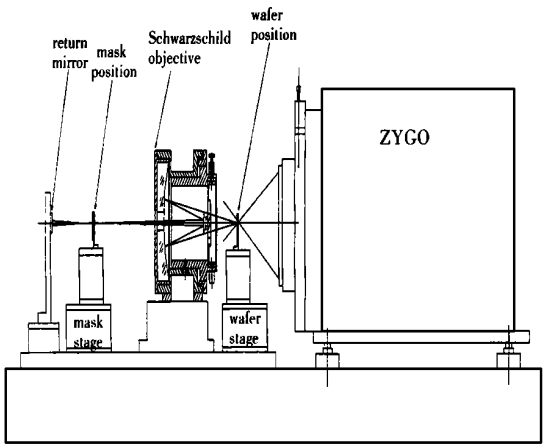

Fig. 11 Arrangement of the computer-aided alignment system

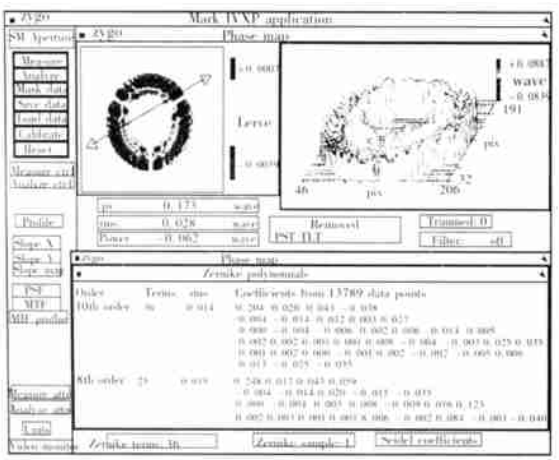

Fig. 12 Wave front errors measured in the final objective

6 Summary and discussion

We have designed an experimental system for the first step investigation of EUVL. It consists of a LPS, an ellipsoid condenser, a transmission mask, and a 10:1 reduction Schwarzschild optics with Mo/Si coated multilayer operating at 13.0nm. The imaging experiments are carried out aiming at resolution about 0.1μm in an image field of 0.1mm in diameter.

In our preparation routine for exposure, we found that the debris spurted out from the copper target contaminated the fused quartz window seriously and also the mask a little, because there was not any shutter or fitter in such operation. It suggests that the utilization of the debris-free target, or specially designed mask could cut most pieces of debris. The main obstacles to our EUVL studies, however, is the restriction in manufacturing technologies. As mentioned above, in our present state the figure error and roughness of the surface (Fig. 6 and Fig. 7) are far from the requirement of high resolution in EUVL. Furthermore, the application of aspherical mirror in EUVL leads to a series of the challenges in optical design, optical polishing and testing of sub-nanometer accuracy in large enough surface scale, multilayer deposition of fine-controlled d spacing, and assembly alignment of off-axis optical system with sub-nanometer wavefront accuracy. These challenges constitute the main research objectives of our lab.

References:

[1] Sweeney Donald W, Russ Hudyma, Chapman, Henty N, et al. EUV optical design for a 100nm CD imaging system[J]. SPIE, 1998, 3331: 2-10.

[2] Kinoshita H, Watanable T, Niibe M, et al. Three-aspherical system for EUVL lithography[J]. SPIE, 1998, 3331: 20-30.

[3] Kubiak G D, Tichenor D A, Malinowski M E, et al. Diffraction-limited soft X-ray projection lithography with a laser plasma source[J]. J. Vac. Sci. Technol, B 9(6): 1991, 3184-3187.

[4] Tichenor D A, Kubiak G D, Haney S J, et al. Recent results in the development of an integrated EUVL laboratory toll [J]. SPIE, 2437: 292-307.

[5] http://www-cxro.lbl.gov/optical_constants/